Poly-Si Etching Using An Electron Cyclotron Resonance Microwave Plasma Sources with Multipole Confinement

S. M. Gorbatkin and L. A. Berry
Oak Ridge National Laboratory
Oak Ridge, Tennessee 37831

CONF-911132--11

DE92 005114

John Swyers*
SEMATECH
Austin, Texas 78741

ABSTRACT

In this study, mirror field and single coil 2.45 GHz electron cyclotron resonance (ECR) microwave plasma sources were coupled to a multipole, multicusp plasma confinement system, and used to produce chlorine plasmas for poly-Si etching. Scanning Langmuir probes were used to study the effect of process parameters on plasma potentials, plasma density, plasma density uniformity, and electron temperature, while poly-Si etching experiments on 150-mm diam wafers were used to relate process parameters and Langmuir probe results to etch rate, SiO_2 selectivity, photo-resist selectivity, and etch uniformity.

RF substrate bias at 13.56 MHz was used for ion energy control, and the addition of a third coil below the substrate plane was found useful for fine-tuning the radial plasma uniformity. Undoped poly-Si etch rates >3000 Å/min, Si/SiO_2 etch selectivities >25, and 150-mm diam etch uniformities <2% at 1 sigma were obtained but not simultaneously. Tradeoffs in choosing operating conditions for optimum poly-Si etch performance will be discussed.

I. INTRODUCTION

Electron Cyclotron Resonance (ECR) microwave ion sources have been increasingly used in recent years for thin film deposition and etching due to their ability to deliver high-current densities (tens of mA/cm^2) at low ion energy (a few tens of eV).[1-3] For etching of polycrystalline Si (poly-Si) for gate electrode formation in integrated circuits, ion energy control is critical since the thin (<100Å) SiO_2 layer below the poly-Si must remain unetched and undamaged while maintaining high etch rates of the poly-Si. Selectivity with respect to the photoresist, also sensitive to the ion energy, is required to be high enough to keep

---

*Present address: Advanced Micro Devices, Austin, TX 78741.

the photoresist intact during the gate formation step. Ion energies <50eV are required to etch Si without etching SiO_2.[4] The presence of carbonateous photoresist fragments in the gas phase complicates process optimization because the etch rates of Si and SiO_2 can be changed if carbon is present at the surface.[5] Uniformity over 150–250-mm diam and profile control (etching square wells with straight walls) are additional requirements for a gate poly-Si etch process.

In this paper, results are presented on Langmuir probe measurements and etch experiments for chlorine plasmas formed in ECR microwave plasma sources. The use of multipole confinement in the ECR system provided uniform 150-mm diam wafer etching over a wide parameter space, however tradeoffs were found between etch rate and selectivity. Langmuir probe measurements provided insight into source behavior and etch response.

II. EXPERIMENTAL APPARATUS AND PROCEDURE

The experimental apparatus used consists of an ASTeX 14.6-cm-ID ECR microwave ion source powered by a 300–1500 W, 2.45 GHz power supply (ASTeX S-1500) connected to a secondary 38-cm-ID anodized Al chamber as shown in Fig. 1. Some experiments were performed with an additional 8.3-cm long, 38-cm ID spool piece whose position is also indicated in Fig. 1. The Al chamber included auxiliary magnets in a multipole configuration similar to a previously described system.[6] Twenty Ceramic-5, 2.9 cm by 2.9 cm by 36.8 cm magnets, with a measured field of ~1 kG within 3 mm of the face were placed with alternating north and south poles facing the 38-cm ID Al chamber. The field at the inside chamber surface was ~700 G. For experiments discussed in Section III-D, the 2-coil mirror plasma source was replaced by a single coil source, with the microwave window attached to a 4.6-cm long, 15-cm ID spool piece on the secondary 38-cm ID Al chamber. Microwave power in the TM_{01} mode was introduced using an ASTeX SPC/F fixed TE_{10} to TM_{01} converter, and a three-stub tuner was used to set the reflected power/forward power to <10%.

The magnetic field for operation at an ECR was provided by two 168 turn, 21.9-cm ID, 33-cm OD, 9.5-cm long coils operated to provide a variety of magnetic field configurations. A third coil (154 turn, 53.2-cm ID, 68-cm OD, 5.1-cm long) positioned near the bottom of the multipole confinement chamber ~86 cm from the microwave entrance window was used for additional B field control. The three coils were typically operated at currents I of I_1 = 160-200 A, I_2 = 80-200 A, I_3 = (-50)-0 A. $I < 0$ indicates a current direction which produces a field opposite that produces by a

positive current. Langmuir probe measurements in the mirror region were performed with 0.051-cm diam, 4-mm-long tungsten cylindrical probes, and measurements in the multipole chamber were performed with 0.025-cm diam, 2-mm long tungsten cylindrical probes. Probe positions are shown in Fig. 1.

The probe I-V curves were analyzed as discussed in Ref 7, and all plasma densities in Figs. 2 and 5 do not include correction factors due to magnetic fields or probe sizes. The expected magnitudes of these corrections range from <10% to 100% and are also discussed in detail in Ref 7. In the etch system, some measurements were performed after processing photoresist-coated wafers, and it was necessary to heat the probes for ~30 sec (while they glowed orange) using a positive 60–100 V bias to drive off the insulating coating.

The space potential P_S was determined by taking the value at the knee of the electron saturation portion of the I-V curve. P_S can also be determined using the equation $P_S = P_f + (kT_e/2q)\ln(m_i/2.3m_e)$, where P_f is the floating potential, T_e is the electron temperature, q is the electron charge, m_i is the ion mass, m_e is the electron mass, and k is Boltzmann's constant.[8] This equation assumes a thermal electron energy distribution. Space potentials determined from this equation will be denoted by $(P_S\text{-}P_f)_{calc}$.

The pressure was measured near the top of the multipole confinement chamber as shown in Fig. 1. Since the capacitance manometer is located in the multipole process chamber behind the auxiliary magnets, the pressure is affected by plasma pumping and gas heating effects.[7,9] To provide a consistent indication of total gas throughput, the pressure was measured and set with the plasma off and will be referred to as $P_{plasoff}$. After setting $P_{plasoff}$, the system was operated at a constant flow with a downstream exhaust valve controller held at a fixed position.

Both patterned and unpatterned wafers were used for the etch characterization. The 150-mm diam substrates were p-type <100> Si with resistivities between 30 and 75 ohm-cm. A thermal oxide of 1000 Å was grown on these substrates, and the oxide was covered by a 4200 Å thick undoped poly-Si layer. Patterned wafers had minimum linewidths of 0.5 μm, with exposed poly-Si after lithography comprising ~50% of the total wafer area.

Etch rates were determined both ex situ, using constant angle reflection interference spectroscopy (CARIS, Prometrix FT-500), or in situ by using the time between minima in the reflected light of a normal incidence 785 nm solid state laser. Two consecutive minima correspond to a thickness of 97.5 nm assuming an index of refraction of 2. In situ values are presented in this paper. Oxide etch rates were

determined ex situ by CARIS, and stylus profilometry was used to measure resist etch rates. Resist etch rates were measured from 200 μm wide square pads on patterned wafers, and oxide etch rates were measured in device-free regions of the patterned wafers with characteristic widths >0.5 mm. The Si/SiO_2 selectivity is given by the ratio of etch rates of Si and SiO_2.

III. RESULTS AND DISCUSSION

A. Uniformity with a 2-Coil Mirror Source

Multipole confinement has been previously used extensively for plasma homogenization.[2,6,10] Even with a multipole confinement system, the specific magnetic field configuration and other operating conditions have a pronounced effect on plasma uniformity. The 150-mm diam uniformities in our systems, as measured by etch response on ~100 unpatterned, undoped poly-Si wafers without an oxide breakthrough step, ranged from well over 100% to <2% at 1 sigma. With a breakthrough step, uniformities as good as 1.3% were achieved. Overall, uniformities better than 5% were available over a broad region of the available parameter space with $P_{plasoff}$ = 0.5–3.0 mTorr, net power = 800–1400 W, and wafer position = 67–83 cm from the microwave entrance window. Furthermore, Langmuir probe measurements indicate comparable uniformity is easily achievable to 200-mm diam in the present configuration. Regions of the parameter space which resulted in nonuniform plasmas were low powers (P <600 W) and/or low pressures ($P_{plasoff}$ <0.2–0.4 mTorr), which yield underdense plasmas,[7] and pressures above ~7 mTorr, which resulted in center peaked plasma density nonuniformities. Additional experiments were performed to study the complete etch response. Section D lists example etch experiments, including specific operating conditions, which yielded 150-mm diam etch uniformities between 1.5 and 34%.

Even though operating parameters such as pressure and/or power could be adjusted to improve uniformity, other etch responses such as etch rate and selectivity would change as well. Varying the third coil current I_3 provides a method of fine tuning plasma density uniformity without dramatically changing other etch responses. For example, Fig. 2 shows that the plasma density uniformity over 200 mm can be improved from 9.4% to 3.1% by increasing the third coil current from -6 to -14 amps. The improvement in uniformity is also accompanied by a 14% increase in plasma density.

The improvements in uniformity and density can be understood by examining Figs. 3a and 3b, which show the change in the 2D magnetic contours and field lines which result from the addition of the opposing third coil current. With increasing third coil current in a direction opposite that of the 1st and 2nd coils, the field lines terminate higher up in the multipole confinement chamber, which increases plasma mixing above the wafer and overall plasma density at the wafer.

Furthermore, the lower magnetic field present at the wafer enhances the ion diffusion coefficient perpendicular to the field lines (D_{perp})[11] which aids homogenization. For example, assuming a thermal ion velocity perpendicular to the field lines of 4×10^4 cm/sec, D_{perp}/D at 1 mTorr increases from 0.02 to 0.2 for a reduction in field strength from 100 G to 30 G. D_{perp} is compared to the ambipolar diffusion coefficient D since for cross field transport, ions lead, whereas for transport along the field, electrons lead with their motion limited by ambipolar fields.

Increased collisions increase cross field transport, and thus D_{perp}/D at 3mTorr is 0.17 and 0.69 at 100G and 30G respectively. The same collisions which increase homogenization, however, decrease the confinement effect of the multipole chamber. Recent work suggests the plasma loss is proportional to the square root of pressure.[12] Our results suggest the multipole chamber is most useful at pressures below 3 mTorr (and at least down to 0.5 mTorr).

For the 2D contours shown in Fig. 3b, optimal uniformity cannot be obtained below the field null (where the field drops to zero and reverses direction). Fig. 4 shows the appearance of a wafer etched 83 cm from the microwave entrance window for the field shown in Fig. 3b. Since field lines connect the wafer surface directly to the cusps of the magnetic field in the multipole confinement chamber, the etch rate is very sensitive to differences in confinement adjacent to N and S poles. The permanent magnets are alternately in and out of phase with the field direction from the solenoidal coils, and thus the pattern has ten spokes of maximum etch rate, half the number of cusps.

B. Etch Rate

Since etching is ion dominated, high-plasma densities will lead to high etch rates. At or near the ECR resonance region, previous studies[7] with Ar have shown that the plasma density close to the ECR absorption region increases monotonically with both power and pressure, however increased collision and recombination rates

at high pressures lead to a decrease in plasma density with increasing pressure if measurements are performed far enough downstream. Measurements of the plasma density as a function of pressure at various positions in the ECR system, shown in Fig. 5, illustrate this effect for Cl_2 plasmas and indicate that the plasma densities near the bottom of the multipole confinement chamber decrease sharply above 2–3 mTorr. High pressures are, however, desirable from the point of view of minimizing the ion energy to maximize the Si/SiO_2 selectivity. Fig. 6 shows plasma potential and Te measurements with downstream probe 4 for the conditions used for the data presented in Fig. 5 which illustrate this.

Without an applied bias, etch rates for the system shown in Fig. 1 were typically 500 Å/min and as high as 780 Å/min. Even taking into account the lower etch rate for undoped poly-Si compared to highly doped or amorphous Si, the etch rates do not meet the 3000 Å/min manufacturing requirement for adequate throughput. Fig. 7 shows the factor of 5 increase in etch rate obtained with an RF bias addition. The x-axis is the induced DC bias measured in the RF matching network through an RF choke. Since there still may be an ion energy distribution about that inferred from this measurement, the x-axis can only be taken as a rough measure of ion energy. The high etch rates are obtained at the expense of selectivity as shown in the next two sections.

C. Etching with a 2-Coil Mirror Source

Table 1 shows the results of a designed experiment used to investigate overall etch response for the 2-coil mirror source coupled to the multipole confinement chamber. The 8.3 cm spool piece (see Fig. 1) was in place for this experiment, and the chuck temperature was maintained at -10°C. The He flow through the chuck was typically 1–3 sccm. The experiment was a Resolution IV fractional factorial of the form $2_{IV}^{(8-4)}$ with one replication.[13] Three wafers were run per treatment combination; one 100% overetched, one 30% overetched, and one partially etched to provide uniformity information. A 30% overetch indicates the 1000 Å thick oxide layer was etched for 30% of the time required to etch through the 4200 Å thick poly-Si layer. The etch rate listed is the average of the three runs, and the oxide etch rate was determined either by using the difference between the 100% and 30% overetch cases divided by the time for 70% overetch, or, in three cases noted, by taking the etch depth for the 100% overetch case. For very low etch rates, a deposit formed on the wafer surface and prevented an accurate measurement of the oxide etch rate.

A complete statistical analysis of the data is beyond the scope of this paper, however a number of features are evident by inspection. One feature is that the uniformities, which are not individually optimized using the third coil and could be further improved by a factor of two or more, are <5.2% in 11 of 17 cases. The etch rate goal of 3000 Å/min is attainable in this configuration, but only with increased ion energy (through both low pressure and high bias) and thus selectivity is generally low.

From the plasma density data presented in Fig. 5, the plasma density at the bottom of the multipole confinement chamber should decrease sharply above 2 mTorr. In fact, the etch rates obtained at 3 mTorr and low bias with the wafer near the probe 4 position were over an order of magnitude lower than the 3000 Å/min required for a practical etch process. Profiles obtained during etch experiments were generally adequate and were not very sensitive to pressure. Some sensitivity to pressure might be expected due to increased gas phase scattering, however in the present case some sidewall passivation from, for example, photoresist fragments may have occurred and decreased dependence of profiles on pressure. Fig. 8 shows a typical profile obtained with net power = 1200 W, Cl_2 flow = 21 sccm, He flow = 9 sccm, $P_{plasoff}$ = 3.0 mTorr, induced bias = -20 V, chuck T = +14 C, I_1 = 160 A, and I_2 = 80 A.

D. Movement to a Single Coil ECR Source

There are two main advantages to moving towards a single coil. The first is a decrease in the unbiased ion energy due to a decrease in the gradient in plasma density. The Boltzman relation for electrons is $n_2 = n_1 \exp(q\phi/kT_e)$ where n_2 and n_1 are the electron densities at two locations and ϕ is the potential gradient formed between them.[14] Thus, assuming no collisions (which is not a good assumption as discussed below), a plasma density gradient of $n_2/n_1 = 25$ at Te = 3 eV would result in ϕ = 10 V. With the single coil source, the resonance is moved into the multipole confinement chamber and can be spread out considerably, reducing the gradient and thus reducing the potential. A second reason, which is believed to dominate, is the increased plasma density present at the wafer surface (per unit power). At low pressures ($\leq 5 \times 10^{-4}$ Torr) the 2-coil mirror improves ionization rates by confining ionizing electrons, but at higher pressures, this effect is less important due to decreased electron mean free paths. The single-coil source yields higher plasma densities at comparable powers due to (1) a shorter distance between the wafer and

the ECR absorption region (see Fig. 5) and (2) less loss to recombination at the source walls, which is a problem for the AsTEX 2-coil mirror source.[15]

Table 2 shows the results of a designed etch experiment which employed the single coil ECR source (current in the single coil = 155 A). The experiment was a resolution IV fractional factorial of the form $2_{IV}^{(6-4)}$ augmented with four center points. Two wafers were etched per treatment combination, one 100% overetched and one partially etched to provide uniformity information Compared to the results presented in Section C, etch rates >~ 3000 Å/min are attainable with a much lower bias, which in turn results in increased selectivites at comparable etch rates. Etch rates between 1000 and 2500 Å/min were obtained with no bias, and Si/SiO_2 selectivities were as high as 105. The uniformity was generally worse than in the 2-coil mirror case, but these experiments were also performed without optimization of the third coil current and thus improvements by a factor of 2-3 are likely.

Recent experiments[16] indicate that above 0.5-1 mTorr in Ar and N_2, any benefit gained from a decrease potential outside the sheath is lost due to collisions, and thus the improvements in etch rate and selectivity seen with the single coil ECR source are believed to be due entirely to an increased plasma density at the wafer surface per unit input power. They may still be benefits, however, from decreasing plasma density gradients at low pressures, and additional Cl cross section measurements are required to more accurately gauge the role of potential drops outside the sheath.

IV. SUMMARY AND CONCLUSIONS

Langmuir probe and etch experiments were performed in chlorine plasmas with either a 2-coil mirror ECR source or a single coil ECR source feeding a multipole multicusp confinement system. The performance of the system was evaluated for use in forming poly-Si gates. Etch uniformities at 1 sigma on 150-mm diam wafers were as low as 1.3% and were generally <5% for pressures between 0.5 and 3 mTorr and powers between 800 and 1400 W under a variety of other operating conditions. Similar uniformity over 8" diameter is expected based on Langmuir probe measurements. The use of a third coil operated with a current, which produced a field opposite that of the source coils, was found especially useful for uniformity control.

Tradeoffs exist in choosing the parameter space for optimum etch performance, especially between etch rate (>3000 Å/min is desired) and Si/SiO_2

selectivity (>50–100 is desired). 3000 Å/min etch rates were obtained, but only with applied RF bias, which increased the ion energy and reduced selectivity to <10. Selectivities up to 105 were obtained for the single coil ECR source, but only with no applied bias and thus with decreased etch rate (<1200 Å/min). The single coil ECR source resulted in improved etch rate and selectivity compared with the 2-coil mirror ECR source and this is believed to be due to an increase in the plasma density present at the wafer surface (per unit power), which is a result of (1) a shorter distance between the wafer and the ECR absorption region, which is especially important above 2 mTorr (see Fig. 5), and (2) less loss due to recombination at the source wall.[15] In these particular experiments, uniformity was worse for the single coil source, but optimization of the field configuration should allow further improvements by a factor of 2-3.

All results discussed in this paper were on undoped poly-Si. The etch rates for heavily doped poly-Si and amorphous Si, often used for gate formation, will be a factor of 2 or more higher. Further improvements in selectivity for the configuration used for this study could be obtained by adding ~0.5–5% O_2 or with other changes in chemistry.[17,18]

ACKNOWLEDEGMENTS

The authors would like to acknowledge the support and encouragement of Jim Roberto throughout this project and thank Gary Henkel for technical support. We also thank Les Jerde, Mitch Carlson, Paul Westerfield, Jack Reece, and Richard Lynch of SEMATECH for invaluable assistance, and Tom Mantei of the University of Cincinnatti for stimulating discussions. This work was sponsored by the Division of Materials Sciences, U.S. Department of Energy under Contract DE-AC05-84OR21400 with Martin Marietta Energy Systems, Inc. and SEMATECH.

REFERENCES

[1]W. M. Holber, "ECR Ion Sources," in *Handbook of Ion Beam Processing Technology*, Ed. by J. J. Cuomo, S. M. Rossnagel, and H. R. Kaufmann (Noyes Publication, Park Ridge, New Jersey1989) p. 21

[2]R. R. Burke, J. Pelletier, C. Pomot, and L. Vallier, *J. Vac. Sci. Technol. A* **8**, (3) 2931 (1990).

[3]J. Musil, *Vacuum* **36**, 161 (1986).

[4]W. M. Holber and J. Forster, *J. Vac. Sci. Technol. A* **8**, (5) 3720 (1990).

[5]S. C. McNevin, *J. Vac. Sci. Technol. A* **9**, (3) 816 (1991).

[6]C. C. Tsai, L. A. Berry, S. M. Gorbatkin, H. H. Haselton, J. B. Roberto, and W. L. Stirling, *J. Vac. Sci. Technol. A* **8**, (3) 2900 (1990).

[7]S. M. Gorbatkin, L. A. Berry, and J. B. Roberto, *J. Vac. Sci. Technol. A* **8**, (3) 2893 (1990).

[8]B. Chapman, *Glow Discharge Processes* (Wiley, New York, 1980), p. 70

[9]S. M. Rossnagel, S. J. Whitehair, C. R. Guarnieri, and J. J. Cumo, *J. Vac. Sci. Technol. A* **8**, (4), 3113 (1990).

[10]Jes Asmussen, *J. Vac. Sci. Technol. A* **7**, (3), 883 (1989).

[11]F. F. Chen, *Introduction to Plasma Physics and Controlled Fusion, Vol I: Plasma Physics* (Plenum Press, New York, 1984) pp. 169–173.

[12]R. Breun, C. Lai, N. Hershkowitz, A. Wendt, and C. Woods, *Multidipole-RF Electrode Experiments*, poster PD-7, 44th Annual Gaseous Electronics Conference, Albuquerque, New Mexico, 10/22–25/91.

[13]G. E. P. Box, W. G. Hunter, and J. S. Hunter, *Statistics for Experimenters, An Introduction to Design Data Analysis, and Model Building,* (John Wiley & Sons, New York, 1978).

[14] F. F. Chen, *Introduction to Plasma Physics and Controlled Fusion, Volume 2: Plasma Physics*, (Plenum Press, New York, 1984) p. 75

[15] S. M. Rossnagel, K. Schatz, S. J. Whitehair, R. C. Guarnieri, D. N. Ruzic, and J. J. Cuomo *J. Vac. Sci. Technol. A* **9**, (3) 702 (1991).

[16] N. Hershkowitz, S. W. Lam, M. Hussein, H Persing, and E. D. Hartog, *What Determines Ion Energy at an Unbiased Wafer in an ECR Etching Tool*, poster JA-1; E. A. D. Hartog, H. Persing, J. S. Hamers, and R. C. Woods, *Laser Induced Fluorescence Studies of Ion Dynamics in an ECR Etcher*, poster DA–1, 44th Annual Gaseous Electronics Conference, Albuquerque, New Mexico, 10/22–25/91.

[17] S. Samukawa, M. Sasaki, and Y. Suzuki, *J. Vac. Sci. Technol. B* **8** (6) 1192 (1990).

[18] S. Samukawa, M. Sasaki, and Y. Suzuki, *J. Vac. Sci. Technol. B* **8** (5) 1062 (1990).

DISCLAIMER

Figure Captions

Fig. 1. Schematic diagram of the etch system used for Cl_2 studies. The AsTEX 2-coil mirror source is shown. The spool piece was used for all 2-coil mirror data presented in this paper except for the plasma measurements in Figs. 5 and 6. The spool piece was not used with the single coil source.

Fig. 2. Plasma density n_i as a function of probe position as measured by downstream probe 3 for two values of I_3. $P_{plasoff}$ = 1.25 mTorr, Cl_2 Flow = 21 sccm, He flow = 2 sccm, net power = 1000 W. I_1 = 180 A and I_2 = 140 A. The axial positions X of the three coils with respect to the microwave entrance window are X_1 = -1.5 cm, X_2 = 29.8 cm, and X_3 = 83.1 cm.

Fig. 3. 2-D magnetic field contours and flux lines for the etch system shown in Fig. 1 with I_1 = 209, I_2 = 128 A, and (a) I_3 = 0, (b) I_3 = -44.6 A. The axial positions X of the three coils with respect to the microwave entrance window are X_1 = 5.6 cm, X_2 = 29.4 cm, and X_3 = 84.7 cm.

Fig. 4. Appearance of an unpatterned poly-Si wafer etched for 4.3 min at an axial position of 83 cm with the field profile shown in Fig. 3b. $P_{plasoff}$ = 0.49 mTorr, Cl_2 flow = 18 sccm, He flow = 2 sccm, net power = 1189 W.

Fig. 5. Plasma density n_i as a function of the pressure with no plasma $P_{plasoff}$ at various positions for the etch system shown in Fig. 1. Net power = 1000 W, Cl_2 flow = 25 sccm, I_1 = 155 A, I_2 = 140 A. The axial positions X of the three coils with respect to the microwave entrance window are X_1 = 2.6 cm, X_2 = 29.4 cm, and X_3 = 76.2 cm.

Fig. 6. Downstream probe 4 measurements of the electron temperature T_e, floating potential P_f, space potential P_s, and calculated difference $(P_s\text{-}P_f)_{calc}$ as a function of $P_{plasoff}$ (the pressure with no plasma) for the conditions used for the data presented in Fig. 5.

Fig. 7. Etch rate on undoped poly-Si patterned wafers as a function of induced DC bias (from an applied RF bias). $P_{plasoff}$ = 1.25 mTorr, net power = 1000 W, Cl_2 flow = 29.5 sccm, He flow = 9 sccm, I_1 = 180 A, I_2 = 140 A, I_3 = -5.4 A. Coil positions were X_1 = 1.8 cm, X_2 = 29.8 cm, and X_3 = 84.7 cm.

Fig. 8. Typical etched profile appearance. $P_{plasoff}$ = 3.0 mTorr, bias = -20 V, net power = 1200 W, Cl_2 flow = 21 sccm, He flow = 9 sccm, chuck temperature = +14°C, I_1 = 160 A, I_2 = 80 A, I_3 = 0 A.

Table 1. Etch Results with 2-Coil Mirror ECR Source.

	Run	Pressure (mTorr)	Bias (Volts)	He Chuck Backside Pressure (Torr)	Power (Watts)	Flow (sccm)	Wafer Position (cm)	Null[a]	B Field Configuration[b] M=Mirror S=Streaming	Si Etch Rate (Å/min)	Uniformity (±% at 1σ)	Si/SiO_2 Selectivity	Si/Resist Selectivity
1	1	1	-60	5	800	20	68	-1	M	2199	2.4	-	1.9
2	8	1	-60	5	800	20	68	-1	M	2215	3.1	5.2	1.6
3	9	3	-60	5	800	40	68	1	S	500	5.2	10.9	1.4
4	11	1	-20	5	800	40	83	1	M	1173	1.5	13.0	1.8
5	15	3	-20	5	800	20	83	-1	S	94	34	Dep[d]	5.9
6	16	1	-60	9	800	20	83	1	S	569	2.0	8.9	1.2
7	14	3	-60	9	800	40	83	-1	M	657	6.9	12.7	1.4
8	10	1	-20	9	800	40	68	-1	S	840	4.1	Dep[d]	2.0
9	6	3	-20	9	800	20	68	1	M	1285	7.2	27.0	2.5
10	2	1	-60	5	1200	40	83	-1	S	1427	2.5	5.8	1.3
11	17	3	-60	5	1200	20	83	1	M	1500	-	6.0[c]	-
12	13	1	-20	5	1200	20	68	1	S	1198	3.0	6.9	2.2
13	5	3	-20	5	1200	40	68	-1	M	1862	3.7	12.5[c]	2.3
14	12	1	-60	9	1200	40	68	1	M	2976	2.6	5.0[c]	2.3
15	4	3	-60	9	1200	20	68	-1	S	1219	5.8	9.6	1.6
16	3	1	-20	9	1200	20	83	-1	M	2006	3.6	7.0	2.9
17	7	3	-20	9	1200	40	83	1	S	163	6.1	Dep[d]	1.6

[a]Null: I_3 = 0% (-1) or I_3 = 75% (1) of the current required for B = 0 at the wafer surface.
[b]B Field: I_1, I_2 = 160, 60 (S) or 180, 140 (M).
[c]Selectivity derived from 100% overetched wafer.
[d]Dep: Indicates deposition on wafer.

Table 2. Etch Results with Single Coil ECR Source.

Run	Null[a]	Pressure (mTorr)	Wafer Power (Watts)	Position (cm)	Bias (Volts)	He Chuck Backside (Torr)	Si Etch Rate (Å/min)	Uniformity (±% at 1σ)	Si/SiO_2 Selectivity
1	1	2.5	1000	83	0	6	1059	3.8	105
2	0	1.75	1200	76	-8	8	2250	7.1	11
3	1	1.0	1400	68	0	9	2250	11.5	36
4	1	1.0	1000	83	-15	9	1430	13.1	14
5	-1	2.5	1400	83	0	9	1238	6.6	22
6	0	1.75	1200	76	-8	8	3000	4.7	14
7	1	2.5	1400	68	-15	6	3162	3.9	5
8	-1	1.0	1000	68	0	6	2053	8.6	39
9	-1	1.0	1400	83	-15	6	2690	5.2	6
10	-1	2.5	1000	68	-15	9	2489	11.2	9
11	0	1.75	1200	76	-8	8	2340	5.4	11
12	-1	2.5	1400	68	0	6	2545	9.1	14
13	-1	2.5	1000	83	-15	6	1603	4.3	13
14	1	2.5	1400	83	-15	9	2600	3.9	9
15	1	2.5	1000	68	0	9	1887	5.0	23
16	1	1.0	1400	83	0	6	1828	16.1	11
17	-1	1.0	1000	83	0	9	1147	4.8	105
18	0	1.75	1200	76	-8	8	2340	5.4	10
19	1	1.0	1000	68	-15	6	2659	5.1	7
20	-1	1.0	1400	68	-15	9	3162	9.2	5

[a]Null: I_3 = 0% (-1), 15% (0), or 30% (1) of the current required for B = 0 at the wafer surface.

Fig. 1

ORNL-DWG 91M-6446R2

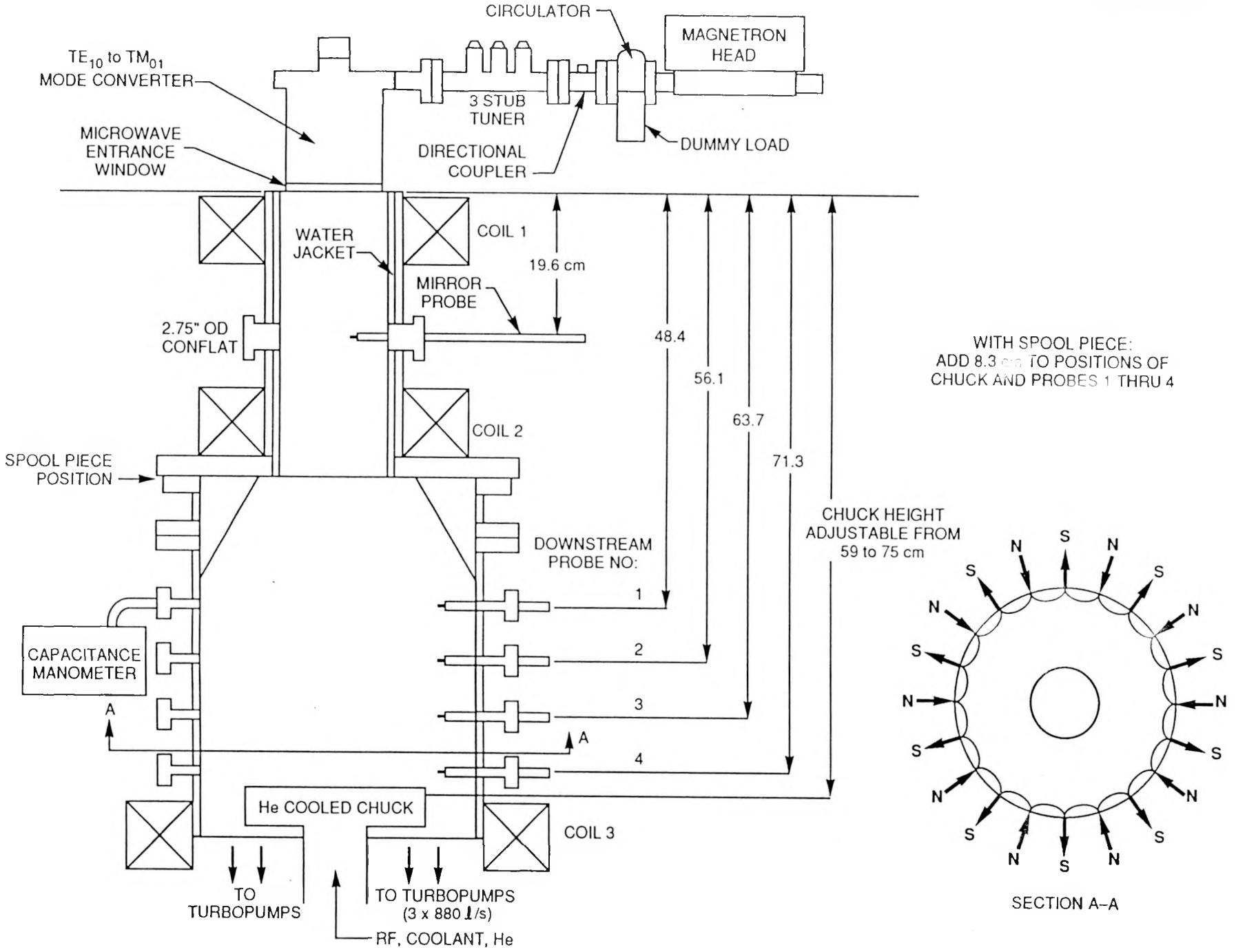

Fig. 2

ORNL-DWG 91M-14881

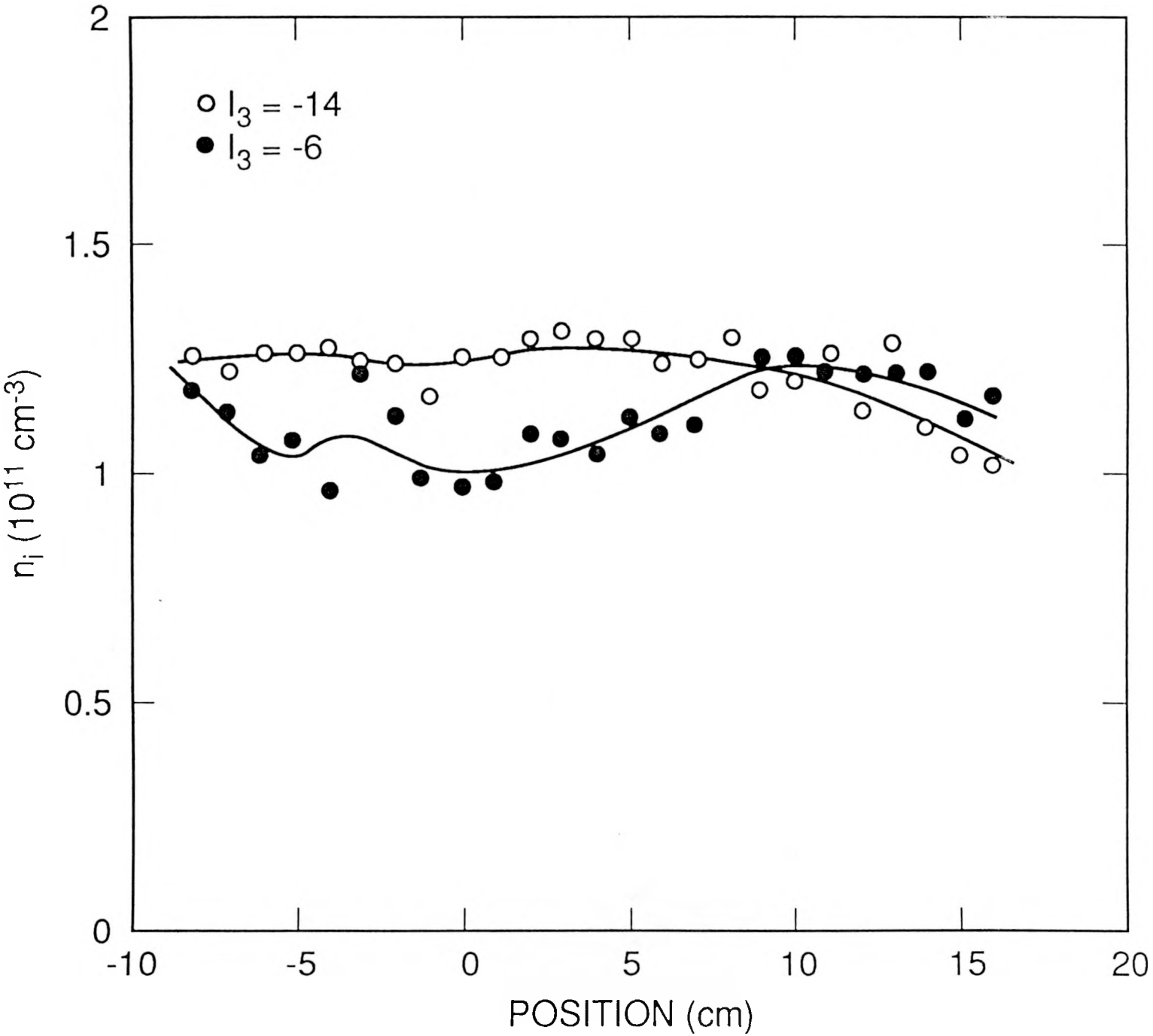

Fig. 3A

ORNL-DWG 91-13180

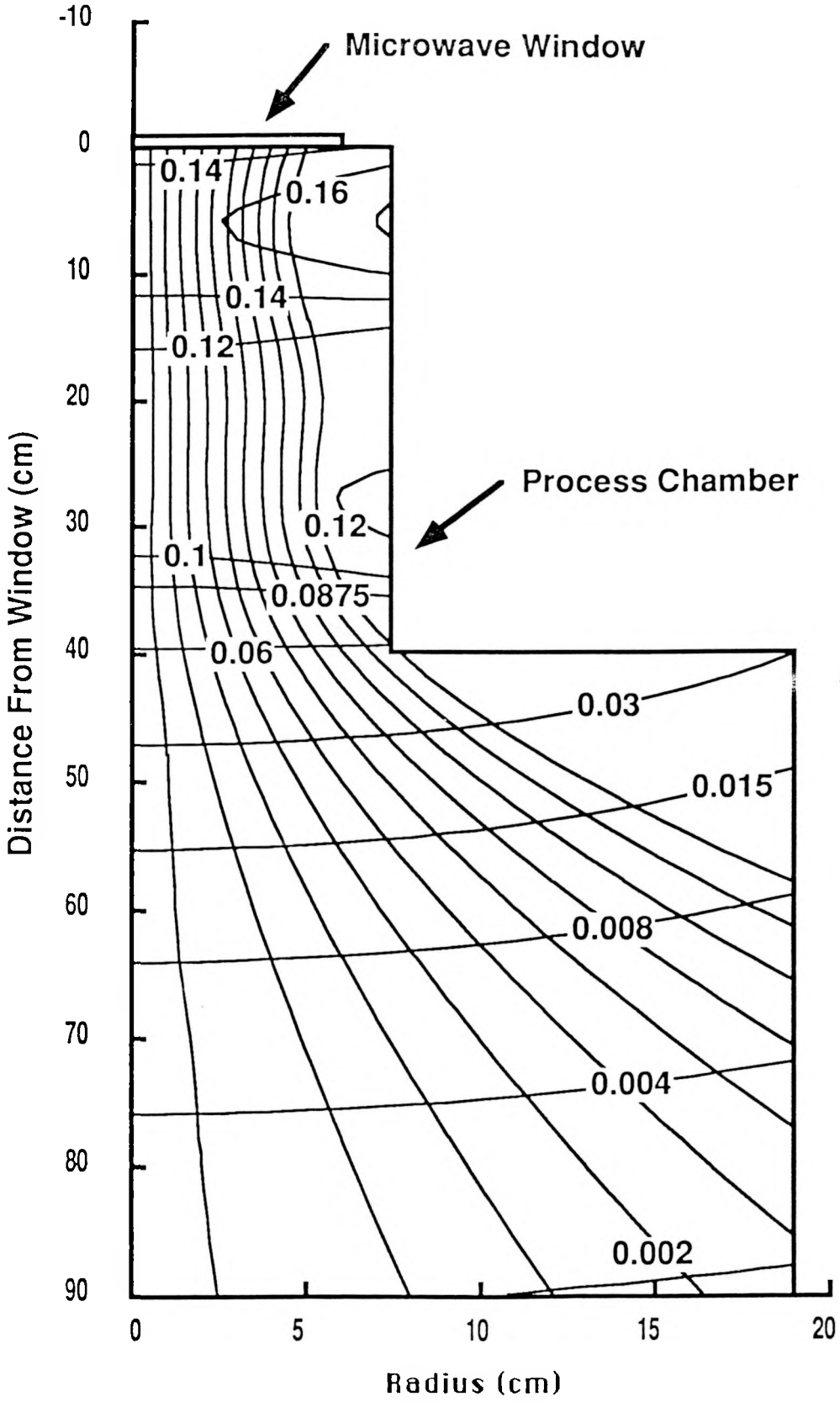

Fig. 3b

ORNL-DWG 91-13179

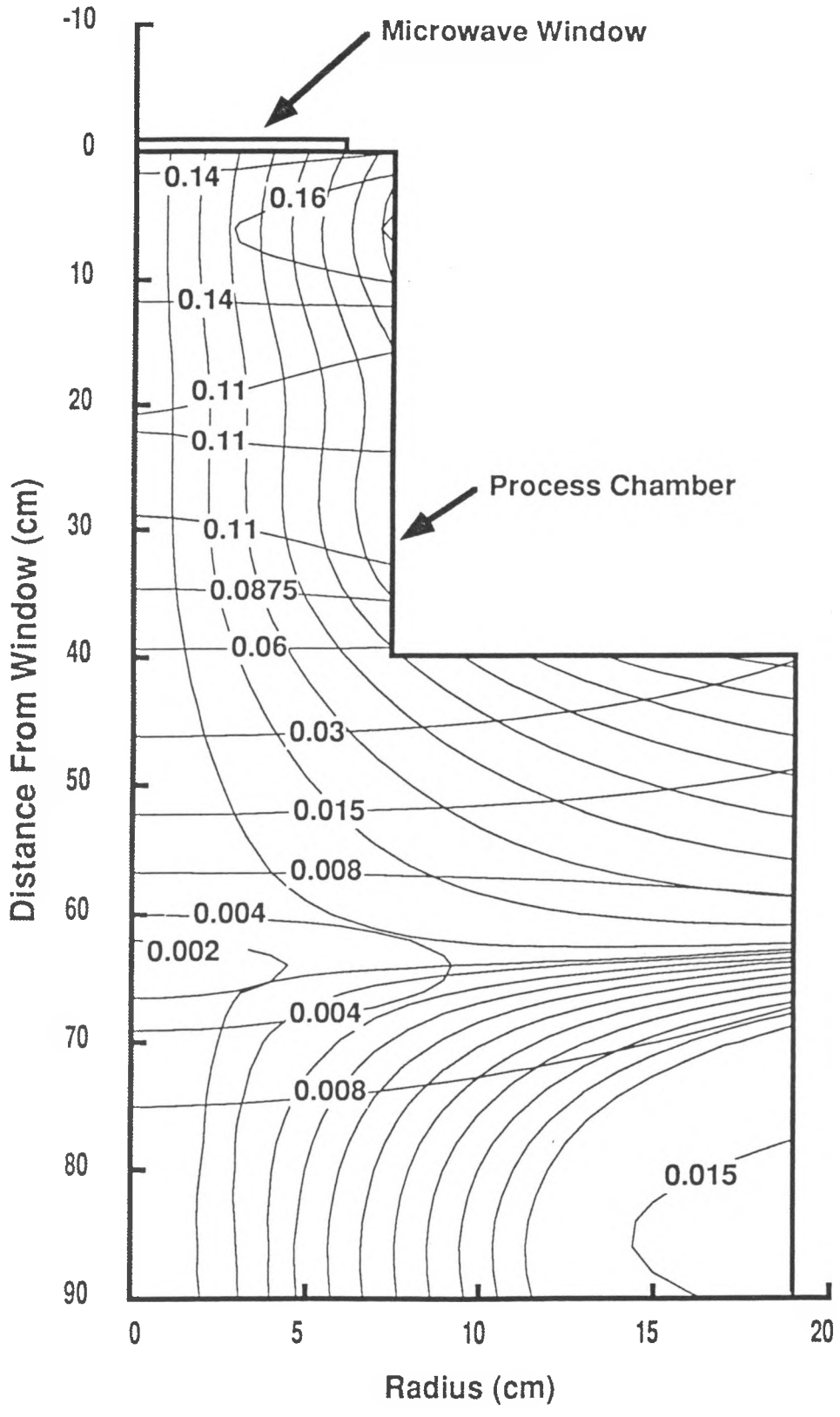

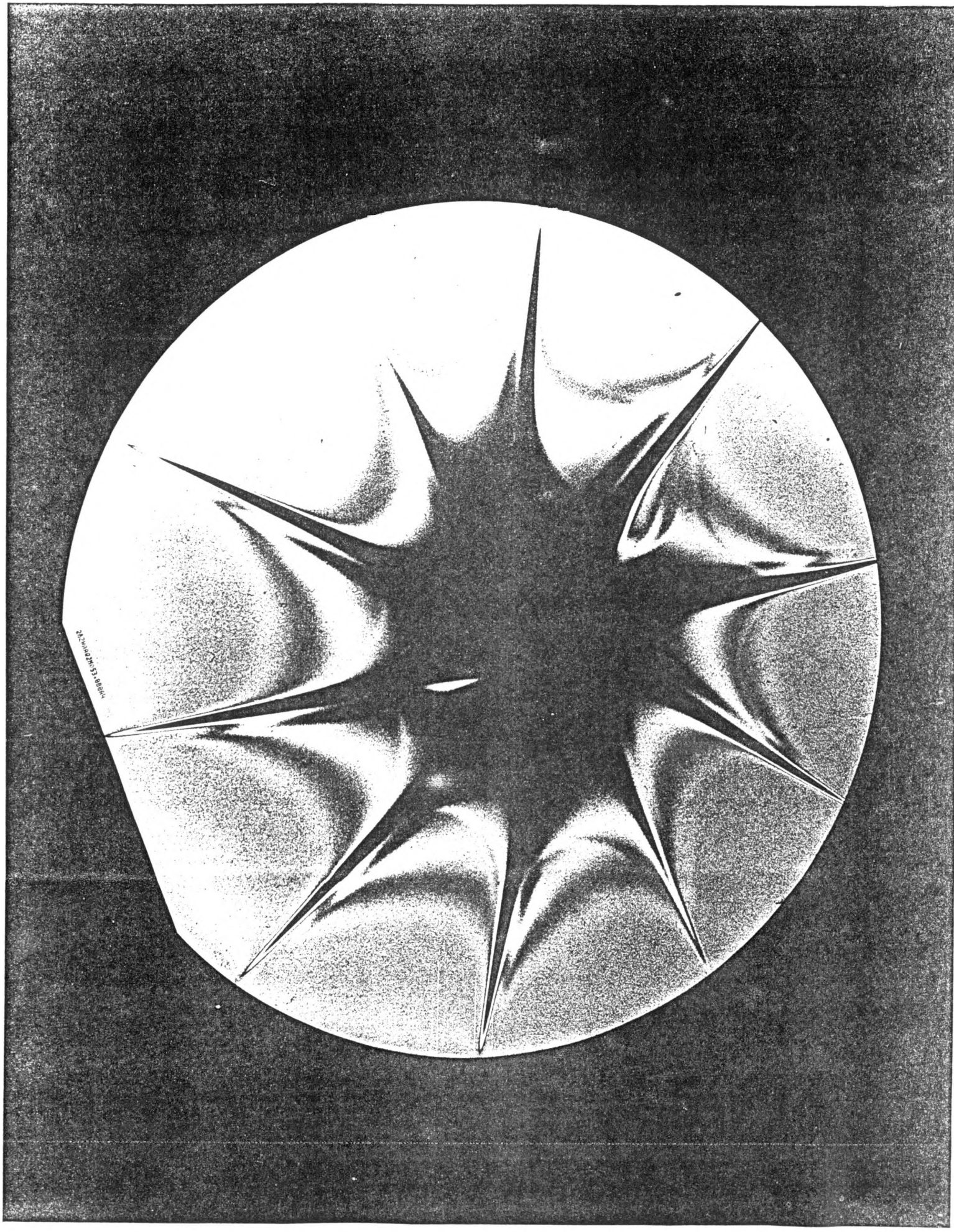

Fig. 4

Fig. 5

ORNL-DWG 91M-14878

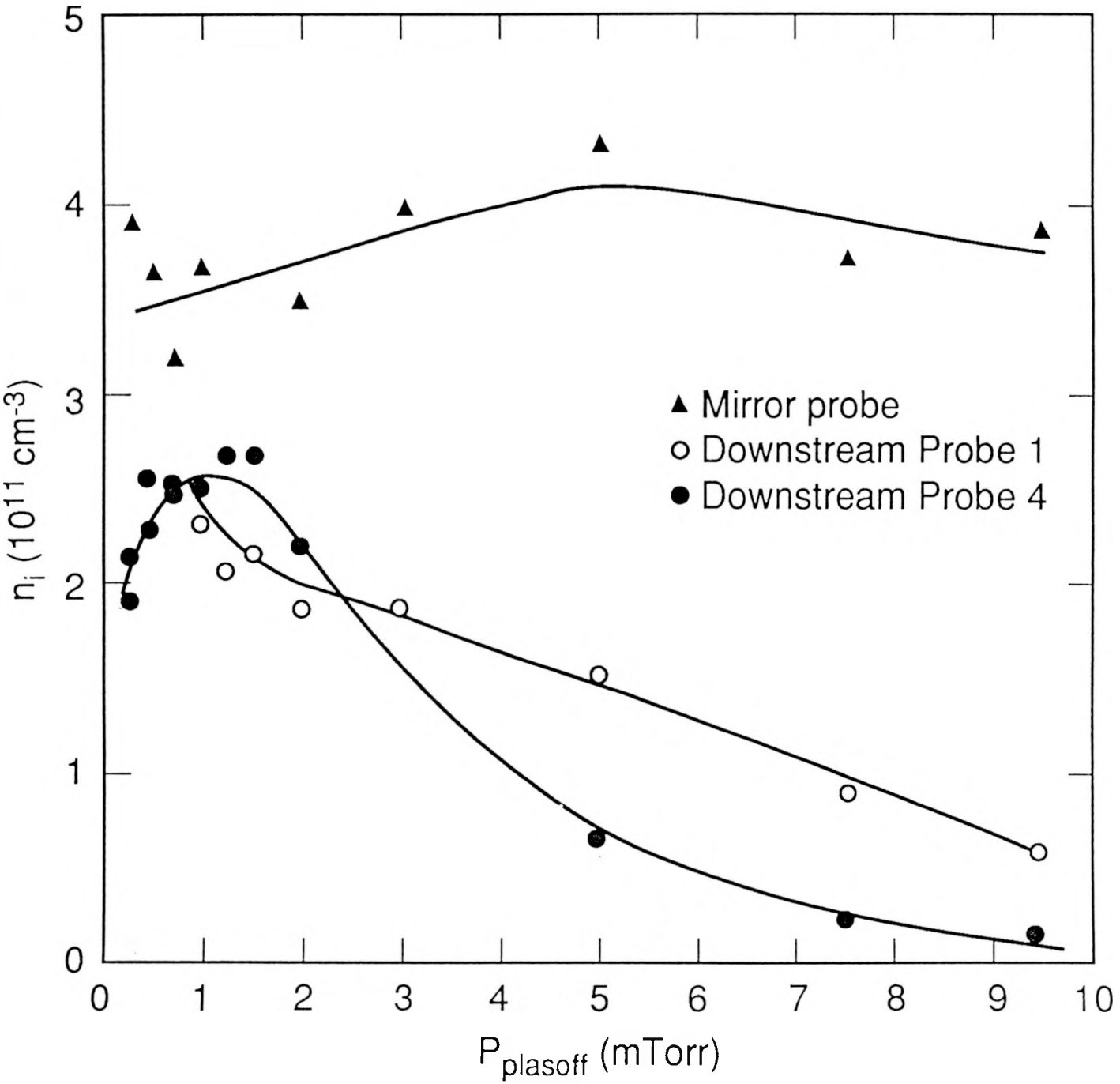

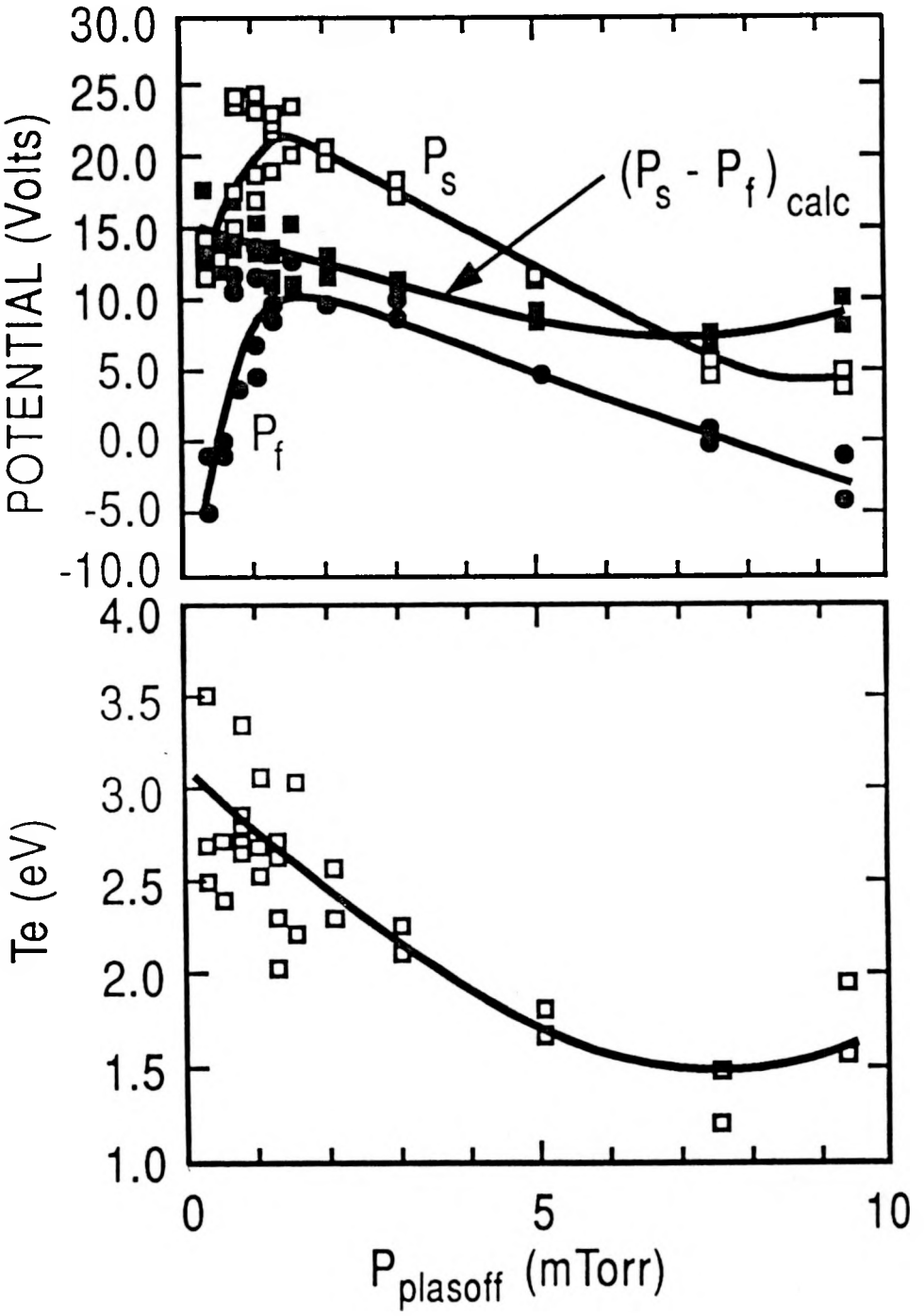
POTENTIAL (Volts)
30.0
25.0
20.0
15.0
10.0
5.0
0.0
-5.0
-10.0
P_s
$(P_s - P_f)_{calc}$
P_f
Te (eV)
4.0
3.5
3.0
2.5
2.0
1.5
1.0
0
5
10
$P_{plasoff}$ (mTorr)

Fig. 7
ORNL-DWG 91M-14880

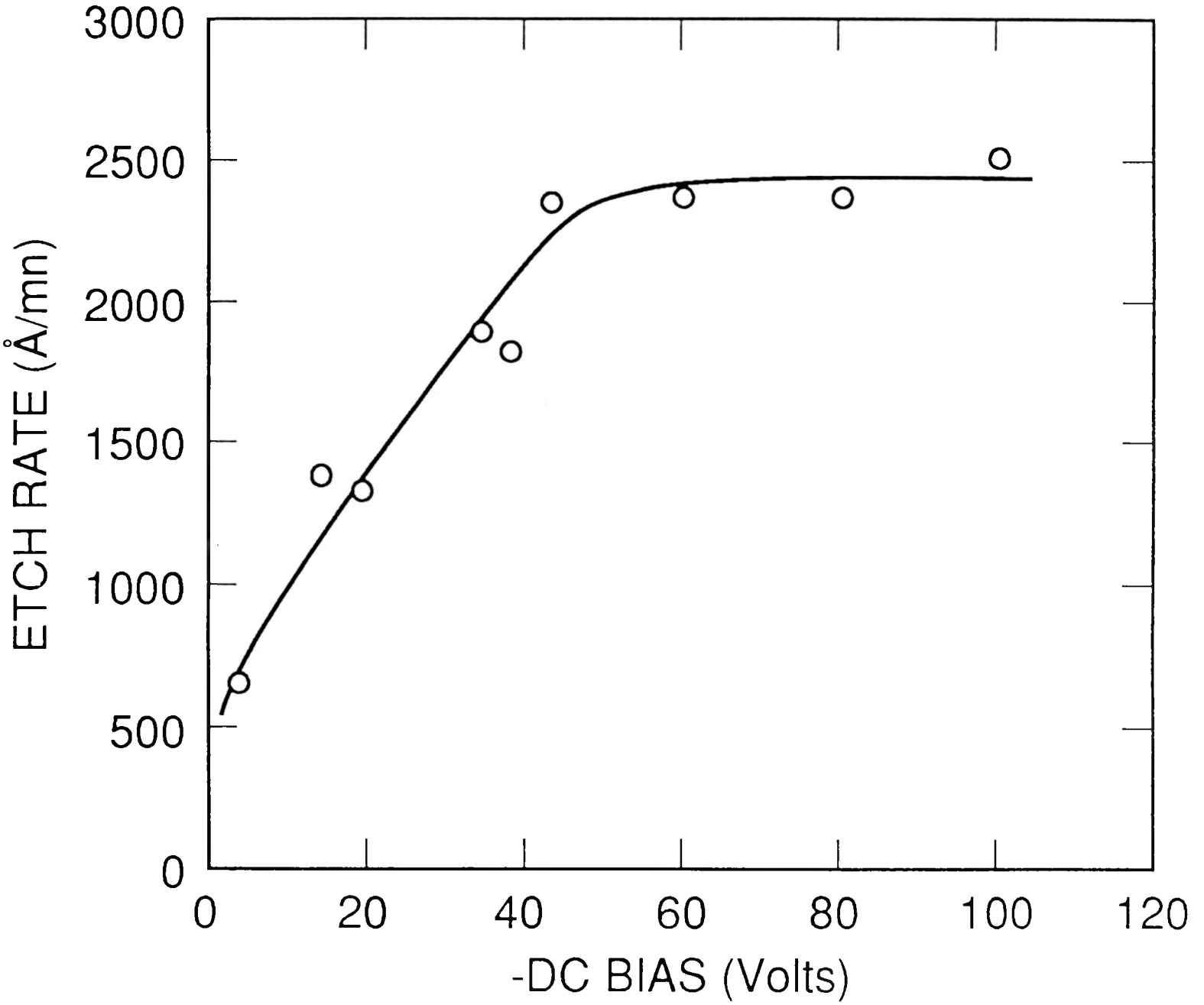

Fig. 8

ORNL-PHOTO 9917-91